

Supporting Information

Co₉S₈ Core-Shell Hollow Spheres for Enhanced Oxygen Evolution Reaction and Methanol Oxidation Reaction by Sulfur Vacancies Engineering

Long Li,^a Zhanpeng Sheng,^a Qingqing Xiao^a, and Qiang Hu^{*a,b}

^a Department of Chemistry, Lishui University, Lishui 323000, P. R. China.

^b Zhejiang Zhentai Energy Technology Co. Ltd, Lishui, 323000, China.

*E-mail: qihu@z-etechnology.cn

1 Materials characterizations

The phase formation was identified using powder X-ray diffraction (XRD) (Bruker D8, Cu-K α). The morphologies of the catalysts were observed by field emission scanning electron microscopy (FE-SEM, HITACHI S-4800) and transmission electron microscopy (TEM, JEOL JEM-2010). The linear scanning energy-dispersive X-ray spectrometry (EDX) and EDX elemental mappings were taken on TEM. The X-ray photoelectron spectroscopy (XPS) spectra were measured on ESCALAB 250 spectrometer (Perkin-Elmer). Raman spectra were analyzed using in-Via Raman spectrometer. The photoluminescence (PL) spectra were obtained by using a Cary Eclipse fluorescence spectrometer (Varian, USA) with Xe lamp as the excitation source. The electron paramagnetic resonance (EPR) spectra were collected at room temperature using a Bruker RPE Elexsys E500 spectrometer equipped with a SHQ with X band frequency in a continuous wave (around 9.8 GHz) cavity. The ICP-OES (PerkinElmer) was used to determine the element contents of the samples.

2 Electrochemical measurements

The electrochemical tests were conducted on CHI 760E electrochemical workstation. The Ag/AgCl (saturated KCl solution) as used as the reference electrode, a graphite rod was served as the counter electrode, and all catalysts were utilized as working electrode.

2.1 Electrochemical OER measurements

All electrochemical tests were performed in 1 M KOH aqueous electrolyte and the catalysts were dissolved in ethanol solution and then uniformly cast onto glassy carbon working electrode with a total loading of 0.4 mg cm⁻². All the linear sweep voltammetry (LSV) measurements were taken at a scan rate of 2 mV s⁻¹ to obtain the polarization curves. Chronoamperometric measurements were performed at corresponding potential to deliver a current density of 10 mA cm⁻². The Tafel slope was calculated according to the Tafel equation $\eta = b \log (j/j_0)$ (η is the overpotential,

b is the Tafel slope, j is the current density, and j_0 is the exchange current density). Potentials were referenced to a reversible hydrogen electrode (RHE) using the following equation: Potentials were referenced to a reversible hydrogen electrode (RHE) using the following equation: $E(\text{RHE}) = E(\text{Ag/AgCl}) + (0.205 + 0.059\text{pH}) \text{ V}$. The double layer capacitance (C_{dl}) was obtained using cyclic voltammetry (CV) scanning from 1.18 to 1.24 V vs. RHE with different scan rates from 20 to 60 mV s^{-1} for OER. The electrochemical impedance spectroscopy (EIS) measurements were carried out by ranging the frequency from 100 k Hz to 0.1 Hz.

2.1 Electrochemical MOR measurements

MOR activities were characterized via cyclic voltammetry (CV) within the potential ranging from 1.0 – 1.8 V vs. RHE at a scan rate of 50 mV s^{-1} . The solution was purged with N_2 for 30 min in prior to each measurement in 1.0 M KOH containing 1 M CH_3OH . The EIS measurements were carried out by ranging the frequency from 100 k Hz to 0.1 Hz in 1 M KOH containing 1 M CH_3OH . Chronoamperometric measurements were performed at corresponding potential to deliver a current density of 40 mA cm^{-2} in 1 M KOH containing 1 M CH_3OH .

2. Supplementary figures

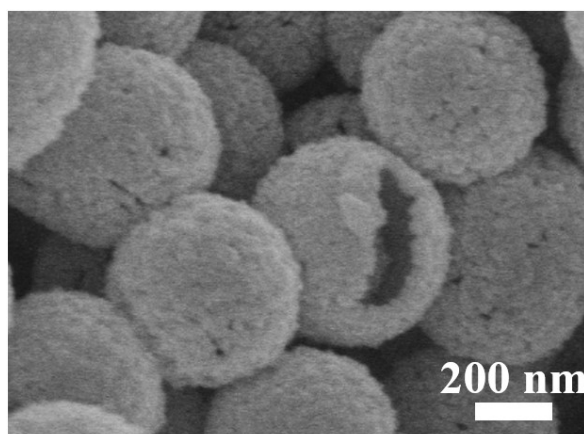


Fig. S1 SEM image of the Co-precursor after sulfidation.

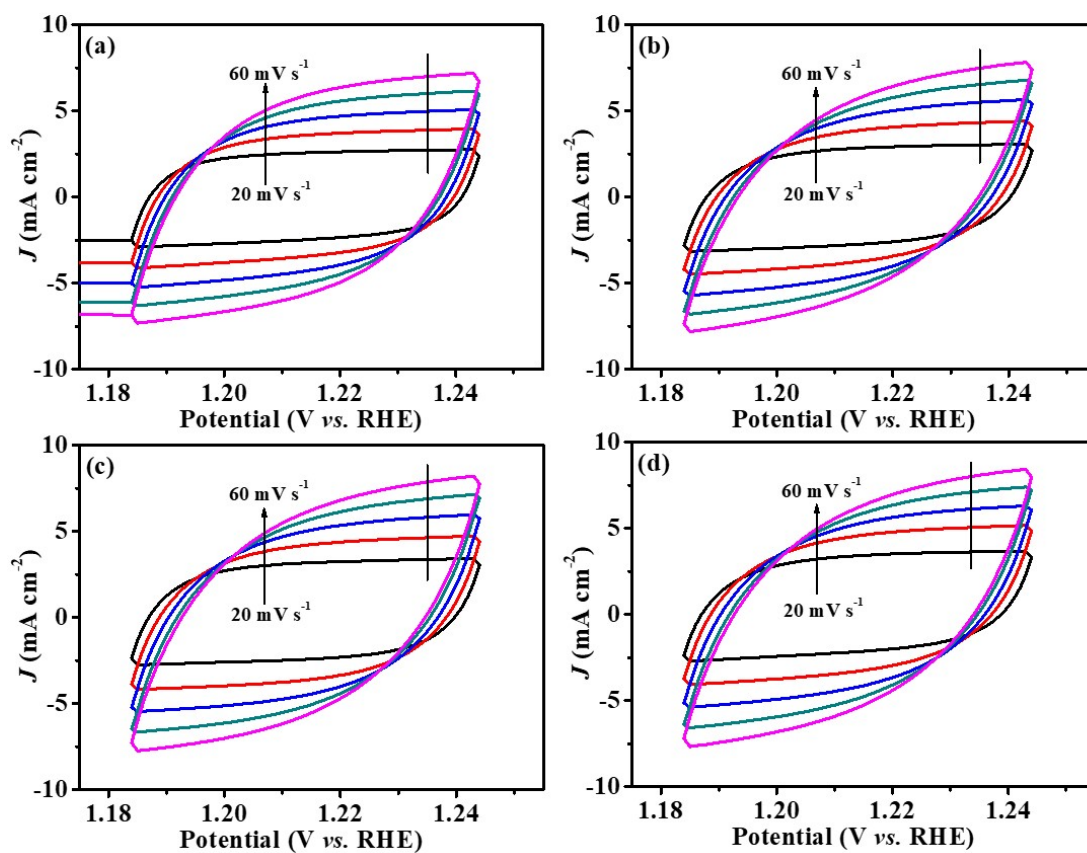


Fig. S2 CVs tested at the potential range of 1.18 –1.24 V vs. RHE with the scan rates increasing from 20 to 60 mV s^{-1} for (a) Co_9S_8 , (b) $\text{Co}_9\text{S}_{8-x}\text{-L}$, (c) $\text{Co}_9\text{S}_{8-x}\text{-M}$ and (d) $\text{Co}_9\text{S}_{8-x}\text{-H}$ spheres.

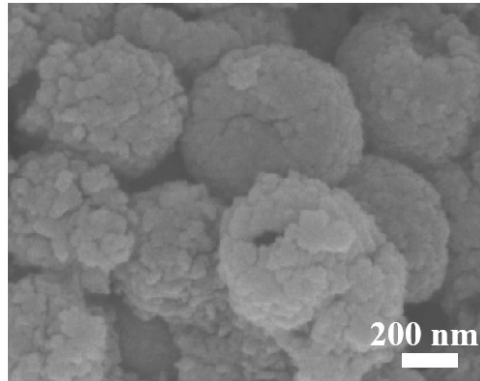


Fig. S3 SEM images of the $\text{Co}_9\text{S}_{8-x}\text{-M}$ spheres after 10 h chronoamperometric test.

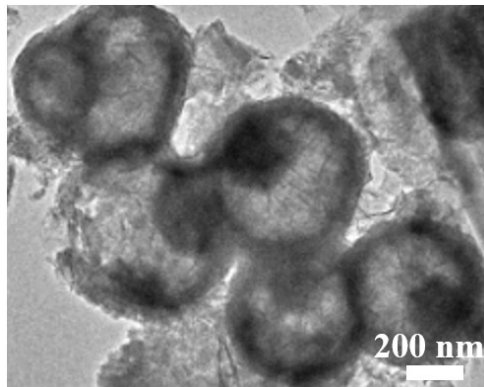


Fig. S4 TEM images of the $\text{Co}_9\text{S}_{8-x}\text{-M}$ spheres after 10 h chronoamperometric test.

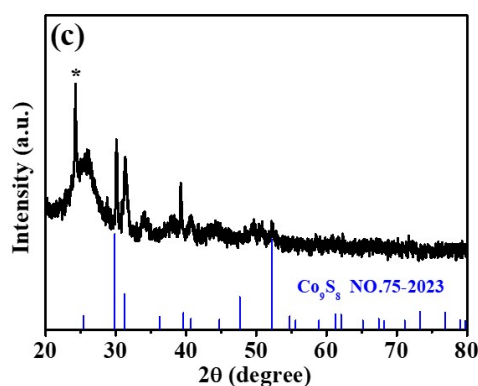


Fig. S5 XRD of the $\text{Co}_9\text{S}_{8-x}\text{-M}$ spheres after 10 h chronoamperometric test.

As shown in the XRD of the $\text{Co}_9\text{S}_{8-x}\text{-M}$ spheres after 10 h chronoamperometric test, a new strong peak at 24° appears, which is correspond to the standard diffraction pattern of CoOOH . The existence of CoOOH in the $\text{Co}_9\text{S}_{8-x}\text{-M}$ spheres after 10 h chronoamperometric test signifies that a part of Co_9S_8 transform into CoOOH during OER process, which is consistent with the transformation reported in the literature.¹⁻³

Table S1 The amount of Co and S, and the ratio of Co-to-S ratio of $\text{Co}_9\text{S}_{8-x}\text{-M}$ spheres.

Sample	amount of Co (mol L^{-1})	amount of S (mol L^{-1})	Co-to-S ratio
$\text{Co}_9\text{S}_{8-x}\text{-M}$ spheres	0.103×10^{-3}	0.088×10^{-3}	9:7.7

The Co-to-S ratio of $\text{Co}_9\text{S}_{8-x}\text{-M}$ spheres is 9:7.7 through ICP-AES, so the cobalt sulfide in this work is Co_9S_8 considering that their XRD characterization is correspond to the standard diffraction pattern of Co_9S_8 (JCPDS 75-2023).

1. J. S. Kim, I. Park, E.-S. Jeong, K. Jin, W. M. Seong, G. Yoon, H. Kim, B. Kim, K. T. Nam and K. Kang, *Adv. Mater.*, 2017, **29**, 1606893.
2. Z. Wang, Z. Lin, J. Deng, S. Shen, F. Meng, J. Zhang, Q. Zhang, W. Zhong and L. Gu, *Adv. Energy Mater.*, 2021, **11**, 2003023.
3. L. Wang, Q. Zhou, Z. Pu, Q. Zhang, X. Mu, H. Jing, S. Liu, C. Chen and S. Mu, *Nano Energy*, 2018, **53**, 270-276.